

## DTA/TG STUDY OF NiO REDUCTION BY Mg+C COMBINED REDUCER

M. K. ZAKARYAN<sup>1,2</sup>, O. M. NIAZYAN<sup>2</sup>, S. V. AYDINYAN<sup>3</sup> and S. L. KHARATYAN<sup>1,2</sup>

<sup>1</sup>A.B. Nalbandyan Institute of Chemical Physics NAS RA  
5/2, P. Sevak Str., Yerevan, 0014, Armenia

<sup>2</sup>Yerevan State University

1, A. Manoukyan Str., Yerevan, 0025, Armenia

<sup>3</sup>Tallinn University of Technology

5, Ehitajate tee, Tallinn, 19086, Estonia

E-mail: zakaryan526219@gmail.com

Kinetic parameters and reaction pathway for the reduction of nickel oxide with simultaneous utilization of magnesium and carbon were established to assess the feasibility of using combined reducers to produce powdered nickel from the NiO-Mg-C system. It was revealed that in this system the reduction of the metal oxide was initiated by Mg, followed by simultaneous action of magnesium and carbon, and at the end of the magnesiothermic process the second stage of the carbothermal reduction started. It was shown that relatively higher heating rates have beneficial influence on the reduction process of nickel oxide. The reduction of nickel oxide by the combined reducer (Mg+C) proceeds at a lower temperature as compared to separate binary mixtures, which evidences of the synergistic effect of combined reducers in the ternary mixture. The activation energy for the NiO+Mg+C reaction ( $117 \text{ kJ}\cdot\text{mol}^{-1}$ ) is lower than that of the binary NiO+C ( $291 \text{ kJ}\cdot\text{mol}^{-1}$ ) and NiO+Mg ( $178 \text{ kJ}\cdot\text{mol}^{-1}$ ) reactions. Thus, the utilization of Mg/C combined reducer allows to mitigate the reduction temperature of NiO, as well as the activation energy compared with the separate carbothermal and magnesiothermic reduction reactions.

Figs. 12, tables 5, references 29.

## 1. Introduction

Preparation of Ni-based alloys with refractory metals, such as tungsten or molybdenum, has been the subject of considerable interest during the past few years. Among such materials, Ni–W alloys exhibit distinguishing mechanical and tribological characteristics which provide enhanced performance for engineering applications. Owing to their superior strength and thermal stability, valuable electric and magnetic properties, high corrosion resistance Ni-W alloys have got increasing consideration in several applications, including protecting and covering coatings,

microelectromechanical systems, magnetic heads and powerful integral schemes. Alloys of tungsten with the metals of iron group (particularly with nickel) are considering as main substitute for hard chromium platings [1-3].

It is well known that alloys containing refractory metal (W, Mo) are inherently difficult to prepare using conventional powder metallurgy due to the large differences in melting points (1455°C and 3422°C for Ni and W, respectively) and limited mutual solubility. Hence, self-propagating high-temperature synthesis (SHS) or combustion synthesis (CS) has been suggested for the preparation of fine Ni-W composite material from oxide precursors by Mg/C combined reducers [4-5] using thermo-kinetic coupling approach [6-7]. However, it is highly challenging to monitor the interaction process in the WO<sub>3</sub>-NiO-Mg-C system and to reveal the mechanism of combustion reaction due to its high velocity. One of the approaches to solve this issue is modeling the process under mild heating conditions (e.g., at low heating rates and tuning the process in time) using the DTA/TG method. By varying heating rates of reagents, it is possible to separate the main stages and analyze intermediate quenched compounds for the efficient exploration of interaction mechanism [8]. Moreover, performing the process with different heating rates allows to use various kinetic schemes developed for this purpose and to calculate kinetic parameters for separate stages.

The implementation of this research enables to obtain kinetic parameters and reduction pathway for the reduction processes of nickel oxide with simultaneous application of magnesium and carbon, with the aim of assessing the feasibility of using combined reducers to produce powdered nickel from the NiO-Mg-C system. Such approach will contribute to the preparation of Ni-W alloys from the NiO-WO<sub>3</sub>-Mg-C system in the combustion mode.

Note that according to the available literature, the mechanism of NiO reduction by the combined Mg/C reducer has not been studied yet. In [9] the reduction of WO<sub>3</sub> was explored by means of combined reducers. The kinetics of nickel oxide reduction into nickel has been studied by using non-metallic reducers due to its practical importance as a catalyst in chemical industry [10-16]. Few kinetic studies have been reported where metals (magnesium or aluminium) were employed directly for the reduction of metal oxides. According to the literature data, high effective activation energy values were obtained for these thermite reactions (CuO+Mg,  $E_a = 424 \pm 25 \text{ kJ}\cdot\text{mol}^{-1}$  [17]; Cu<sub>2</sub>O+Al,  $E_a = 658 \text{ kJ}\cdot\text{mol}^{-1}$  [18]; MoO<sub>3</sub>+Al,  $E_a = 209\text{-}373 \text{ kJ}\cdot\text{mol}^{-1}$  [19];  $E_a = 312 \text{ kJ}\cdot\text{mol}^{-1}$  for the Al-30%Mg+Fe<sub>2</sub>O<sub>3</sub> reaction [20]).

In our previous studies in the CuO-Mg-C [21], WO<sub>3</sub>-Mg-C [9, 22], MoO<sub>3</sub>-Mg-C [21, 23] systems at low and high heating rates the use of Mg+C reducing mixture was found attractive, especially due to the crucial influence of carbon addition on a reaction pathway with a lower effective activation energy.

This study is motivated by the need to investigate the interaction behavior and kinetic features of the NiO-Mg, NiO-C and NiO-Mg-C systems in non-isothermal conditions using DTA/TG method. Based on the data obtained interactions in the NiO-Mg-C system and in more complicated NiO-WO<sub>3</sub>-Mg-C system can be

controlled allowing to fabricate powdered nickel or Ni-W alloys using the advanced combustion synthesis method.

## 2. Materials and methods

The experiments were carried out by differential thermal (DTA) and thermogravimetric (TG) analysis methods using Q-1500 instrument (Derivatograph Q1500 MOM, Hungary) which is linked to multichannel acquisition system, and output signals are recorded by a computer. The reactive powder mixture (30-200 mg) is placed into one of two crucibles. In the second crucible the  $\text{Al}_2\text{O}_3$  powder is placed, which is used as a reference material. All measurements were conducted in nitrogen flow ( $100\text{-}120\text{ ml}\cdot\text{min}^{-1}$ ). Heating rate was programmed to be 2.5, 5, 10,  $20^\circ\text{C}\cdot\text{min}^{-1}$ . In order to reveal the reaction mechanism, the process was terminated at preset temperatures, and the samples were cooled down in inert gas flow. Phase compositions of the intermediate and final products were analyzed by X-ray diffraction (XRD; D5005, Bruker, USA) using  $\text{CuK}\alpha 1$  radiation ( $\lambda = 1.5406\text{ \AA}$ ) with a step of  $0.02^\circ$  ( $2\theta$ ) and a count time of 0.4 s.

As raw materials nickel (II) oxide (reagent grade, Russia, TU 6-09-4125-80), magnesium (MPF-3, Russia, pure, particle size  $0.15\text{ mm} < \mu < 0.3\text{ mm}$ ), carbon (P-803, Russia,  $\mu < 0.1\text{ }\mu\text{m}$ ) were used in experiments.

## 3. Results and discussion

To clarify the interaction mechanism in the complex ternary (NiO-Mg-C) system, it was expedient firstly to explore the reaction pathways in the binary (NiO-Mg, NiO-C) systems in the identical conditions of linear heating.

### 3.1. NiO-Mg binary system

Fig. 1 depicts DTA/TG curves of the NiO+Mg stoichiometric mixture. It is clear that strong exothermic reduction starts before the melting point of magnesium ( $650^\circ\text{C}$ ), when temperature exceeds  $630^\circ\text{C}$  (heating rate:  $V_h = 10^\circ\text{C}\cdot\text{min}^{-1}$ ,  $m_o = 50\text{ mg}$ ). A single stage process occurs and the maximum shift of the DTA curve appears at  $T_{\text{max}} = 648.3^\circ\text{C}$ . It must be emphasized that no mass change was registered during the process. The latter is a clear fact that the reaction proceeds by solid+solid scheme ( $\text{NiO} + \text{Mg} = \text{Ni} + \text{MgO}$ ) and no evaporation of reagents takes place (Fig. 1, TG curve).

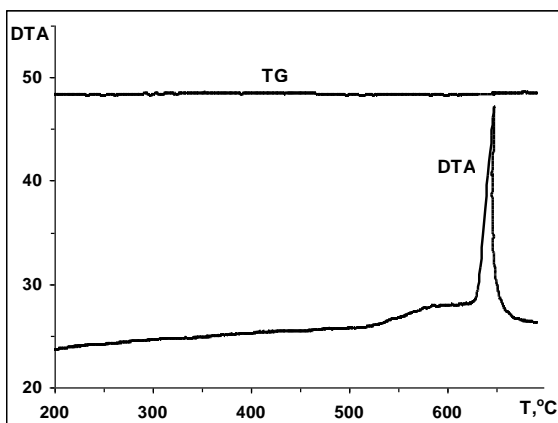


Fig. 1. DTA/TG curves of the NiO+Mg mixture,  $V_h = 10\text{ }^\circ\text{C}\cdot\text{min}^{-1}$ ,  $m_o = 50\text{ mg}$ .

To reveal the influence of heating rate on the interaction mechanism, the DTA/TG studies were performed at heating rates from 2.5 up to  $20\text{ }^\circ\text{C}\cdot\text{min}^{-1}$ . As it can be seen from the figure 2, with the increasing of heating rate, exothermic peaks of magnesiothermic reduction of nickel oxide shift to higher temperature area. In parallel, the intensity of DTA peaks increases. Thus, in the case of  $V_h = 2.5\text{ }^\circ\text{C}\cdot\text{min}^{-1}$  it is weakly expressed, while peaks at  $V_h = 5, 10, 20\text{ }^\circ\text{C}\cdot\text{min}^{-1}$  demonstrate the character of explosive reactions (Fig. 2; Table 1).

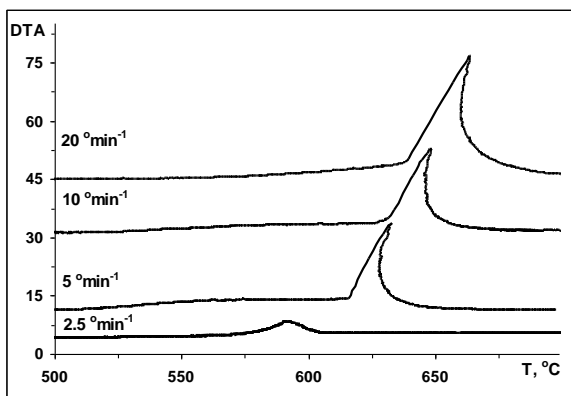


Fig. 2. DTA curves of the NiO+Mg mixture at various heating rates:  $V_h = 2.5; 5; 10; 20\text{ }^\circ\text{C}\cdot\text{min}^{-1}$ .

Table 1

**Influence of heating rate on the temperature range and  $T_{\max}$  for the NiO+Mg system**

Heating rate, $^\circ\text{C}\cdot\text{min}^{-1}$	Reduction temperature range, $^\circ\text{C}$	$\text{DTA}_{\max}$ , $^\circ\text{C}$
20	635-715	663.7
10	630-670	648.3
5	615-652	631.7
2.5	570-610	593.3

In all cases, the main process predominately occurs before melting of Mg and the interaction takes place with a solid + solid mechanism. To some extent, the

reaction with relatively high heating rate ( $20^{\circ}\text{C}\cdot\text{min}^{-1}$ ) deviates from this scheme (Table 1). In this case, the interaction begins with participation of solid Mg but lasts up to a temperature surpassing the melting point of Mg.

According to the results obtained at different heating rates, the latter phenomenon strictly affects the reduction degree. Thus, with increasing the heating rate, the intensity of Ni peaks in the XRD pattern (for the samples cooled down from  $700^{\circ}\text{C}$ ) noticeably increases; in parallel, the intensity of NiO peaks decreases (Fig. 3). Therefore, relatively higher heating rates have beneficial influence on the magnesiothermic reduction of nickel oxide.

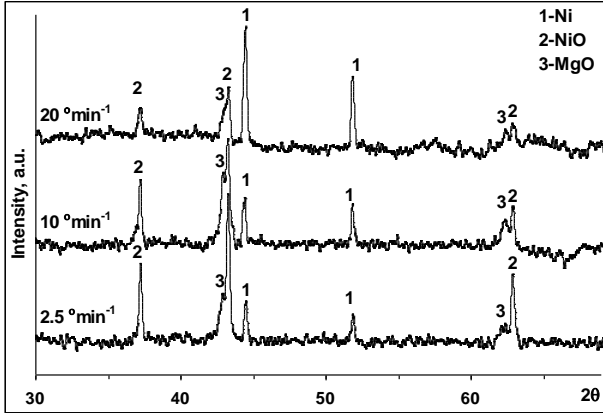


Fig. 3. XRD patterns of the NiO+Mg reaction products at various heating rates.

### 3.2. NiO-C binary system

Experiments in the NiO-C binary system reveal that at linear heating ( $V_h = 10^{\circ}\text{C}\cdot\text{min}^{-1}$ ,  $m_o = 200\text{ mg}$ ) the stepwise carbothermal reduction is registered. Fig. 4 shows that there are no significant changes in the reactive mixture up to  $750^{\circ}\text{C}$ . When the temperature exceeds  $750^{\circ}\text{C}$  an endothermic reduction is registered with two sequential stages, which is simultaneously noticeable on DTA, TG and DTG curves. At that, the second stage is more intensive (Fig. 4). Note that in [24-26] was also reported that nickel oxide carbothermal reduction at high-temperature area occurred by two macroscopic stages.

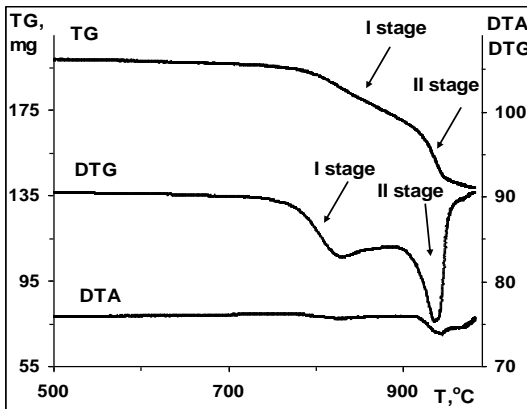


Fig. 4. DTA/TG/DTG curves of the NiO+C mixture,  $V_h = 10^{\circ}\text{C}\cdot\text{min}^{-1}$ ,  $m_o = 200\text{ mg}$ .

The mass change in the TG curve corresponds to the release of carbon dioxide or/and carbon monoxide either during the first or second stage of the process:



According to mass loss calculations, the carbothermal reduction degree increases with the increase of the heating rate (Table 2). For example, according to the results shown in Fig. 4, the mass loss makes about 31% (according to the above reaction equation: 32.3%).

Table 2

**Influence of heating rate on the initial mixtures' mass loss**

Heating rate, $^{\circ}\text{C}\cdot\text{min}^{-1}$	Mass loss by C, %
20	31.3
10	31.0
5	29.2
2.5	17.5

As can be seen from Fig. 5 (DTG curves), nickel oxide reduction by carbon proceeds at different temperature ranges depending on the heating rate. With the increase of the heating rate, the reduction process shifts to a higher temperature area (Table 3).

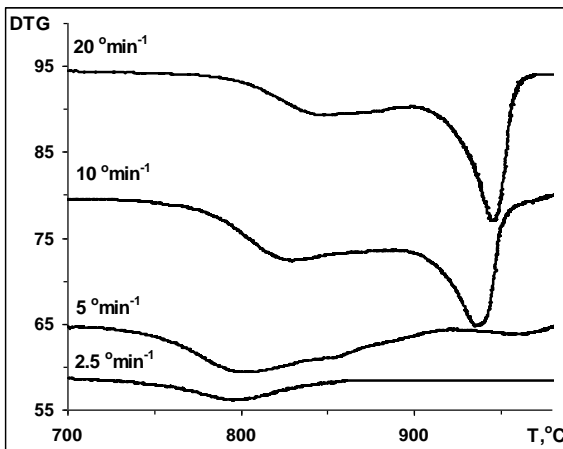


Fig. 5. DTG curves of the NiO+C mixture at various heating rates.

Table 3

**Influence of heating rate on the temperature range and  $T_{\text{max}}$  for the NiO+C system**

Heating rate, $^{\circ}\text{C}\cdot\text{min}^{-1}$	Reduction temperature range, $^{\circ}\text{C}$		$(\text{DTG}_{\text{min}})$ , $^{\circ}\text{C}$	
	I stage	II stage	I stage	II stage
20	780-900	905-985	843.4	948.1
10	750-890	900-970	829.5	943.3
5	730-930	935-990	808.6	966.2
2.5	715-860	—	782.6	—

As it was mentioned above, carbothermal reduction degree increases with the increase of the heating rate. This has been also proved by the results of XRD analysis of the reduction products at the end of the process (Fig. 6): with the increase of heating rate, the nickel oxide carbothermal reduction degree increases as it was in the case of magnesiothermic reduction.

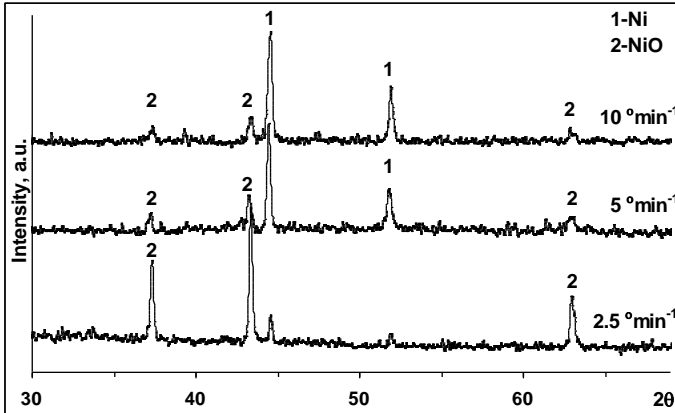


Fig.6. XRD patterns of the NiO+C reaction products at various heating rates.

### 3.3. NiO-Mg-C ternary system

Finally, thermal analysis in ternary NiO-Mg-C system was performed with the  $2\text{NiO}+\text{Mg}+\text{C}$  stoichiometric mixture to distinguish carbon and magnesium reduction processes during the external heating. The DTA/TG curves in Figure 7 illustrate that first exothermic conversion proceeds at  $590\text{--}740^\circ\text{C}$  ( $T_{\text{max}} = 673.5^\circ\text{C}$ ), which corresponds to the  $\text{NiO} + \text{Mg} = \text{Ni} + \text{MgO}$  reaction (see Fig. 8). In the DTA curve, the endothermic process of magnesium melting is also observed. TG and DTG curves show the mass loss expressed in two different segments (Fig. 7) validating that the carbothermic reduction of nickel oxide is a double-stage process [24-26]. The first decline in the TG curve starts at  $625^\circ\text{C}$  ( $\text{DTG}_{\text{min}}$  is observed at  $684^\circ\text{C}$ ), slightly later than the magnesiothermic process starts ( $590^\circ\text{C}$ ). The second decline starts at  $740^\circ\text{C}$  ( $\text{DTG}_{\text{min}}$  is observed at  $853.7^\circ\text{C}$ ), simultaneously with the end of the magnesiothermic process. This indicates that in the NiO-Mg-C system the reduction of the metal oxide is initiated by Mg (including magnesium melting zone), followed by simultaneous action of magnesium and carbon, and at the end of the magnesiothermic process, the second stage of the carbothermal reduction starts. The latter is additionally proved by XRD patterns of the samples cooled down at different temperatures (Fig. 8).

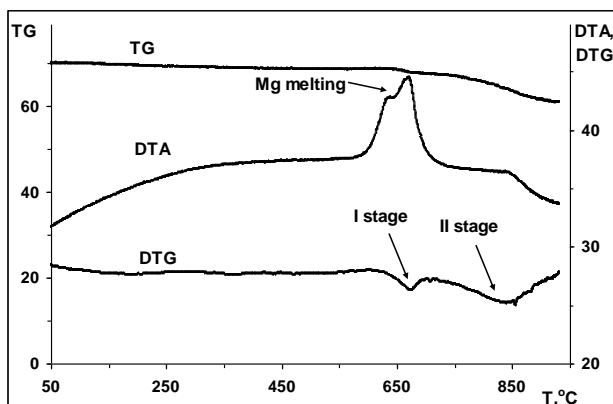


Fig. 7. DTA/TG/DTG curves of the 2NiO+Mg+C mixture,  $V_h = 20^\circ\text{C}\cdot\text{min}^{-1}$ ,  $m_o = 70\text{ mg}$ .

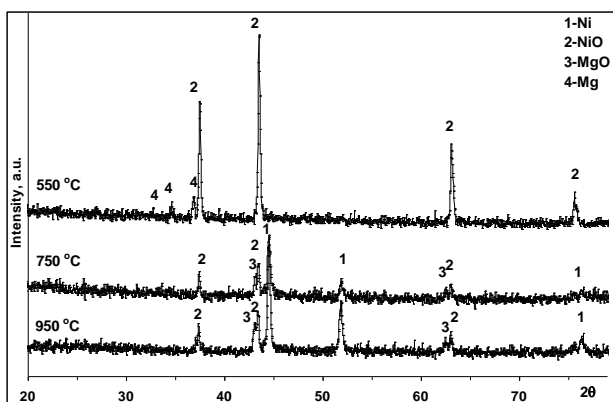


Fig. 8. XRD patterns of the 2NiO+Mg+C reaction products cooled down from different temperatures.

The results obtained during examinations of NiO reduction by combined Mg/C reducer are substantially different from the NiO reduction behavior by individual reducers. Here we deal with a typical example of the reactions kinetic coupling. According to the data obtained from individual reduction processes, the magnesiothermic reduction of nickel oxide (at  $V_h = 20^\circ\text{C}\cdot\text{min}^{-1}$ ) proceeds at 635-715°C temperature range with  $\text{DTA}_{\text{max}} = 663.7^\circ\text{C}$ . In the case of the same heating rate the carbothermal reduction occurs at 780-900°C; 905-985°C temperature ranges ( $\text{DTG}_{\text{mins}}$  are observed at 843.4 and 948°C, respectively). So, the magnesiothermic reduction in the ternary system starts earlier by 50°C than in the NiO-Mg system, and the carbothermal two-stage reduction process moves to a low temperature area by 160 (I stage) and 60°C (II stage). Thus, the reduction of nickel oxide by the combined reducer (Mg+C) proceeds at lower temperatures as compared to separate binary mixtures, which evidences of the particular synergistic effect in the ternary mixture.

According to the mass loss calculations, the carbothermal reduction degree in the ternary system increases with the increase of the heating rate. Thus, according to the reaction equation ( $\text{NiO} + \text{Mg} + \text{C} \rightarrow \text{Ni} + \text{MgO} + \text{CO}/\text{CO}_2\uparrow$ ), the maximum value of mass loss conditioned by carbothermal reduction process is 15.2%. On the

other hand, during the different heating rates in the reduction process the following percentages of weight loss were observed: 1.02% at  $2.5^{\circ}\text{C}\cdot\text{min}^{-1}$ , 5.32% at  $5^{\circ}\text{C}\cdot\text{min}^{-1}$ , 7.92% at  $10^{\circ}\text{C}\cdot\text{min}^{-1}$  and 11.76% at  $20^{\circ}\text{C}\cdot\text{min}^{-1}$ . These results suggest that despite the degree of metal reduction increases with the increase of heating rate, carbon does not provide complete reduction of nickel oxide at least up to a temperature of  $950^{\circ}\text{C}$  (Fig. 9).

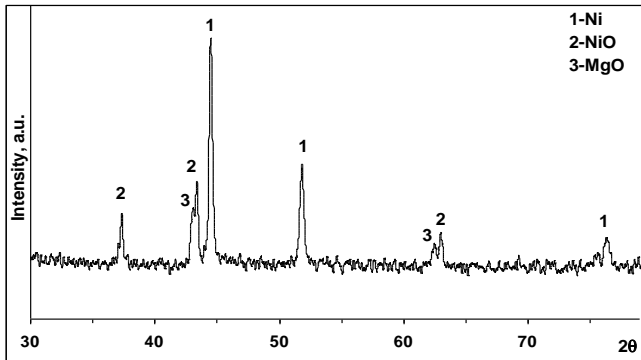


Fig. 9. XRD pattern of the  $2\text{NiO}+\text{Mg}+\text{C}$  reaction product,  $T = 950^{\circ}\text{C}$ ,  $V_h = 20^{\circ}\text{C}\cdot\text{min}^{-1}$

As in the case of binary systems, in the ternary NiO-Mg-C system exothermic peaks of nickel oxide magnesiothermic reduction also shift to the higher temperature area (Table 4, Fig. 10)

Table 4

**Influence of heating rate on the temperature range and  $T_{\text{max}}$  for the  $2\text{NiO}+\text{Mg}+\text{C}$  system**

Heating rate, $^{\circ}\text{C}\cdot\text{min}^{-1}$	Reduction temperature range, $^{\circ}\text{C}$	(DTA <sub>max</sub> ), $^{\circ}\text{C}$
20	590-740	673.5
10	570-680	626.2
5	550-660	592.8
2.5	520-600	570.2

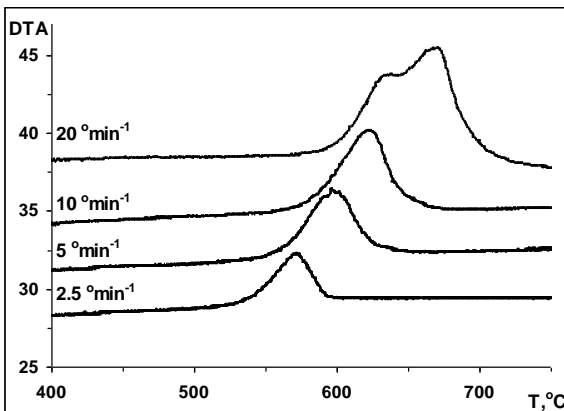


Fig. 10. IDTA curves of the  $2\text{NiO}+\text{Mg}+\text{C}$  mixture at various heating rates.

### 3.4. Calculation of activation energy

Based on the results obtained by DTA/DTG/TG investigations the effective activation energy values were calculated for the reduction stages for all the studied reactions. There are several approaches for calculation of the effective activation energy in non-isothermal conditions. Among them are the well-known isoconversion methods formulated by Kissinger [27] and Ozawa [28]. Both methods are based on the shift of temperature corresponding to the maximum advance in the DTA (Kissinger) and DTG (Ozawa) curves depending on the heating rate kept constant. The methods are based on the Arrhenius equation corrected for the nonisothermicity of the reaction in such a way, that the temperature is a function of time.

The derived expression for determination of activation energy by Kissinger has the following form:

$$\ln\left(\frac{V_h}{(T_{max}^{DTA})^2}\right) = \ln A - \frac{E}{R}\left(\frac{1}{T_{max}^{DTA}}\right)$$

and by Ozawa method the following form:

$$\ln\left(\frac{V_h}{(T_{max}^{DTG})^2}\right) = \ln A - \frac{E}{R}\left(\frac{1}{T_{max}^{DTG}}\right)$$

where, A is a constant, E is the effective activation energy of the process, ( $\text{kJ}\cdot\text{mol}^{-1}$ ),  $V_h$  is the heating rate ( $\text{K}\cdot\text{min}^{-1}$ ),  $T_{max}$  is the reduction temperature corresponding to the maximum advance in the DTA/DTG curve (K), R is the universal gas constant.

#### 3.4.1. Magnesiothermic and magnesiocarbothermal reduction of NiO (Kissinger method)

In Figure 11, experimental data for the reduction of nickel oxide by Mg (1) and Mg+C (2) mixture in appropriate coordinates are summarized. Based on these plots the values of effective activation energy are calculated. Thus, the activation energy for NiO + Mg reaction is  $178 \text{ kJ}\cdot\text{mol}^{-1}$  and for NiO + (Mg+C) reaction -  $117 \text{ kJ}\cdot\text{mol}^{-1}$  (refers to the magnesiothermic stage) (Fig. 11).

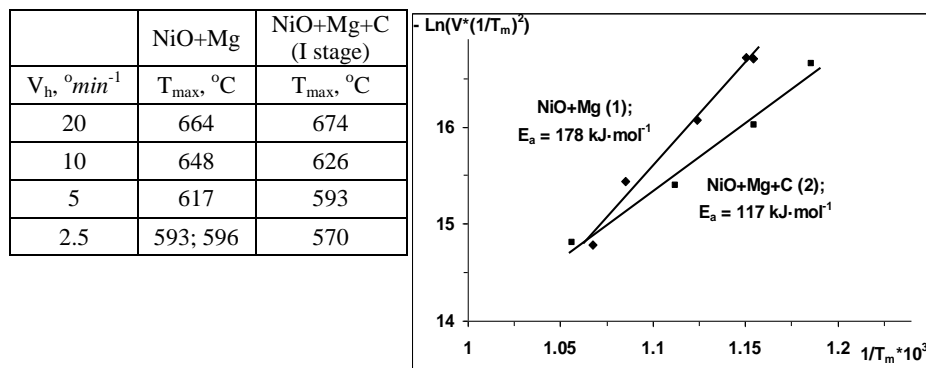


Fig. 11. Determination of activation energy values for NiO+Mg (1) and NiO+Mg+C (2) reactions by Kissinger method.

In comparison, according to [9], the activation energy for (WO<sub>3</sub>+Mg) reaction is 153 *kJ·mol<sup>-1</sup>* and for (WO<sub>3</sub>+Mg+C) is 177 *kJ·mol<sup>-1</sup>* (refers to the magnesiothermic reduction stage), while for (CuO+Mg) reaction is 424 *kJ·mol<sup>-1</sup>* [17] (Table 5).

### 3.4.2. Carbothermal reduction of NiO (Ozawa method)

In Figure 12 experimental data in appropriate coordinates for the reduction of nickel oxide by carbon are summarized. According to Figure 12, the activation energy for NiO reduction by carbon is 291 *kJ·mol<sup>-1</sup>*. In comparison, in [29] for nickel oxide carbothermal reduction the activation energy value was determined to be 299 *kJ·mol<sup>-1</sup>* (Table 5).

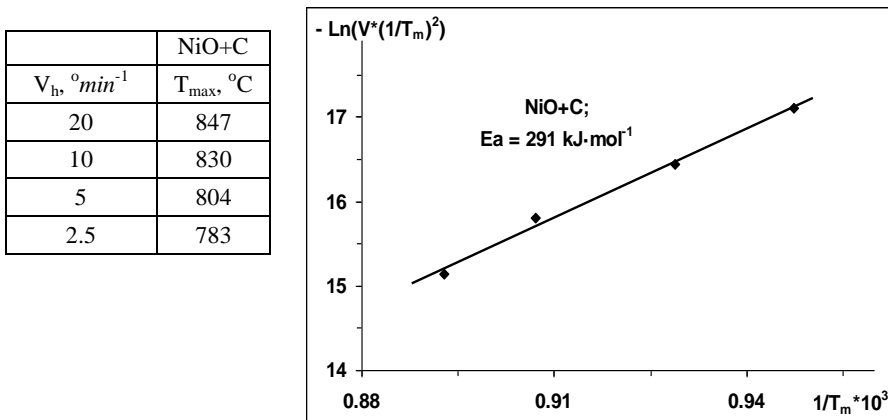


Fig. 12. Determination of activation energy for NiO+C reaction by Ozawa method.

Table 5

### Comparison of the values of activation energies with reference data

Reaction	Activation energy, <i>kJ·mol<sup>-1</sup></i>	Reference
WO <sub>3</sub> + Mg	153	[8]
CuO + Mg	424	[16]
WO <sub>3</sub> + Mg + C (for WO <sub>3</sub> + Mg)	177	[8]
NiO + C	299	[28]
NiO + Mg	178	[this work]
NiO + Mg + C (for NiO+Mg)	117	[this work]
NiO + C	291	[this work]

Furthermore, the activation energy of nickel oxide reduction by carbon is comparable with that of the same reaction determined from isothermal experiments (315 *kJ·mol<sup>-1</sup>*) [25].

Thus, the activation energy for the NiO+Mg+C reaction (117 *kJ·mol<sup>-1</sup>*) is lower than that of the binary NiO+C (291 *kJ·mol<sup>-1</sup>*) and NiO+Mg (178 *kJ·mol<sup>-1</sup>*) reactions.

The application of Mg/C combined reducer allows to decrease the activation energy of magnesiothermic reduction stage by about 1.5 times.

## **NiO-ի ՎԵՐԱԿԱՆԳՆՄԱՆ ՊՐՈՅԵՍԻ ՈՒՍՈՒՄՆԱՍԻՐՈՒԹՅՈՒՆԸ Mg+C ՆԱՄԱԿՑՎԱԾ ՎԵՐԱԿԱՆԳՆԻՉՈՎ ԴԵՐԻՎԱՏՈԳՐԱՖԻԱԿԱՆ ԵՂԱՆԱԿՈՎ**

**Մ. Կ. ԶԱԲԱՐՅԱՆ, Օ. Մ. ՆԻԱԶՅԱՆ, Ս. Վ. ԱՅԳԻՆՅԱՆ և Ս. Լ. ԽԱՌԱՏՅԱՆ**

*Սույն աշխատանքում ուսումնասիրվել են Mg/C համակցված վերականգնիչով նիկելի օքսիդի վերականգնման կինետիկական օրինաչափությունները դերիվատոգրաֆիական եղանակով գծային տաքացման պայմաններում: Բացահայտվել է, որ NiO-Mg-C համակարգում նիկելի օքսիդի վերականգնումն սկսվում է մագնեզիումով, շարունակվում է միաժամանակ մագնեզիումով և ածխածնով, իսկ մագնեզիումաջերմային պրոցեսի ավարտին զուգահեռ սկսվում է ածխածնով վերականգնման երկրորդ փուլը: Հաստատվել է, որ տաքացման արագության մեծացումը բարենպաստ ազդեցություն ունի նիկելի օքսիդի վերականգնման աստիճանի վրա: Ցույց է տրվել, որ նիկելի օքսիդի վերականգնումը Mg/C վերականգնիչով տեղի է ունենում համեմատաբար ավելի մեղմ ջերմաստիճանային պայմաններում՝ համեմատած NiO+Mg և NiO+C բինար համակարգերի հետ, ինչը վկայում է սիներգետիկական էֆեկտի մասին: Որոշվել են հետազոտված ուսուցիչների էֆեկտիվ ակտիվացման էներգիայի արժեքները, որոնք NiO+Mg+C, NiO+C և NiO+Mg ուսուցիչների համար համապատասխանաբար կազմել են 117, 291 և 178 կՋ/մոլ<sup>-1</sup>:*

## **ДТА/ТГ ИССЛЕДОВАНИЕ ВОССТАНОВЛЕНИЯ NiO КОМБИНИРОВАННЫМ ВОССТАНОВИТЕЛЕМ Mg+C**

**М. К. ЗАКАРЯН<sup>1,2</sup>, О. М. НИАЗЯН<sup>1</sup>, С. В. АЙДИНЯН<sup>3</sup> и С. Л. ХАРАТЯН<sup>1,2</sup>**

<sup>1</sup> Институт химической физики им. А.Б. Налбандяна НАН Республики Армения

Армения, 0014, Ереван, ул. П. Севака, 5/2

<sup>2</sup> Ереванский государственный университет

Армения, 0025, Ереван, ул. А. Манукяна, 1

<sup>3</sup> Таллинский технологический университет

Эитайате ул. 5, Таллинн, 19086, Эстония

E-mail: zakaryan526219@gmail.com

В данной работе дериватографическим методом исследованы кинетические закономерности восстановления оксида никеля (II) комбинированным восстановителем Mg/C в условиях линейного нагрева. Установлено, что восстановление NiO начинается магнием, продолжается одновременно магнием и углеродом, а в конце магниетермического процесса наступает вторая стадия карботермического восстановления. Выявлено, что увеличение скорости нагрева оказывает благотворное влияние на степень восстановления окиси никеля. Показано, что восстановление оксида никеля (II) комбинированным восстановителем (Mg+C) происходит при более низких температурах по сравнению с отдельными бинарными смесями NiO+Mg и NiO+C, что свидетельствует о наличии синергетического эффекта. Определены значения эффективной энергии активации исследованных реакций: 117 кДж·мол<sup>-1</sup> – для реакции NiO+Mg+C, 291 кДж·мол<sup>-1</sup> – для NiO + C и 178 кДж·мол<sup>-1</sup> – для NiO + Mg.

## REFERENCES

- [1] *Eliaz N., Sridhar T.M., Gileadi E.* // *Electrochim. Acta*, 2005, v. 50, p. 2893.
- [2] *Younes O., Gileadi E.* // *J. Electrochem. Soc.*, 2002, v. 149, №2, p. 100.
- [3] *Aning A.O., Wang Z., Courtney T.H.* // *Acta Metall. Mater.*, 1991, v. 4, p. 165.
- [4] *Merzhanov A.G.* // *J. Mater. Chem.*, 2004, v. 14, p. 1779.
- [5] *Varma A., Rogachev A.S., Mukasyan A.S., Hwang S.* // *Adv. Chem. Eng.*, 1998, v. 24, p. 79.
- [6] *Merzhanov A.G.* // *Int. J. SHS*, 2011, v. 20, p. 61.
- [7] *Kharatyan S.L., Merzhanov A.G.* // *Int. J. SHS*, 2012, v. 21, p. 59.
- [8] *Baghdasaryan A.M., Niazyan O.M., Khachatryan H.L., Kharatyan S.L.* // *Int. J. Refract. Met. Hard Mater.*, 2015, v. 451, p. 315.
- [9] *Baghdasaryan A.M., Niazyan O.M., Khachatryan H.L., Kharatyan S.L.* // *Int. J. Refract. Met. Hard Mater.*, 2014, v. 43, p. 216.
- [10] *Alizadeh R., Jamshidi E., Ebrahim H.A.* // *Chemical Engineering & Technology*, 2007, v. 30, №8, p. 1123.
- [11] *Richardson J.T., Scates R., Twigg M.V.* // *Applied Catalysis A: General*, 2003, v. 246, №1, p. 137.
- [12] *Szekely J., Evans J.W.* // *Metall. Mater. Trans. B*, 1971, v. 2, №6, p. 1699.
- [13] *Evans J.W., Song S., Leon-Sucre C.E.* // *Metall. Mater. Trans. B*, 1976, v. 7, №1, p. 55.
- [14] *Szekely J., Lin I.* // *Metall. Trans.*, 1975, v. 7, №3, p. 493.
- [15] *Rostrup-Nielsen J.R.* // *PCCP*, 2001, v. 3, p. 283.
- [16] *Gong M., Zhou W., Tsai M.C., Zhou J., Guan M., Lin M.C., Zhang B., Hu Y., Wang D.Y., Yang J., Pennycook S.J.* // *Nature communications*, 2014, v. 5, p. 4695.
- [17] *Hosseini S.G., Sheikhpour A., Keshavarz M.H., Tavangar S.* // *Thermochim. Acta*, 2016, v. 626, p. 1.
- [18] *Wang L.L., Munir Z.A., Maximov Y.M.* // *J. Mater. Sci.*, 1993, v. 28, p. 3693.
- [19] *Schoenitz M., Umbrajkar S., Dreizin E.L.* // *J. Propul. Power*, 2007, v. 23, №4, p. 683.
- [20] *Wang Y., Jiang W., Zhang X., Liu H., Liu Y., Li F.* // *Thermochim. Acta*, 2011, v. 512, №1-2, p. 233.
- [21] *Kirakosyan H., Minasyan T., Niazyan O., Aydinyan S., Kharatyan S.* // *J. Therm. Anal. Calorim.*, 2016, v. 123, p. 35.
- [22] *Aydinyan S.V., Nazaretyan Kh.T., Zargaryan A.G., Tumanyan M.E., Kharatyan S.L.* // *J. Therm. Anal. Calorim.*, 2018, v. 133, №1, p. 261.
- [23] *Manukyan Kh., Aydinyan S., Aghajanyan A., Grigoryan Y., Niazyan O., Kharatyan S.* // *Int. J. Refract. Met. Hard Mater.*, 2012, v. 31, p. 28.
- [24] *Sharma S.K., Vastola F.J., Walker P.L.* // *Carbon*, 1996, v. 34, №11, p. 1407.
- [25] *Sharma S.K., Vastola F.J., Walker P.L.* // *Carbon*, 1997, v. 35, № 4, p. 529.
- [26] *Sharma S.K., Vastola F.J., Walker P.L.* // *Carbon*, 1997, v. 35, № 4, p. 535.
- [27] *Kissinger H.E.* // *Anal. Chem.*, 1957, v. 29, №11, p. 1702.
- [28] *Ozawa T., Kato T.* // *J. Therm. Anal.*, 1991, v. 37, p. 1299.
- [29] *Grigoryan E.G., Niazyan O.M., Kharatyan S.L.* // *Kinet. Catal.*, 2018, v. 48, p. 829.